Nanoscale Res Lett (2010) 5:38–47
DOI 10.1007/s11671-009-9440-5

NANO EXPRESS

Hall Measurements on Carbon Nanotube Paper Modified With Electroless Deposited Platinum

Leslie Petrik · Patrick Ndungu · Emmanuel Iwuoha

Received: 15 June 2009 / Accepted: 9 September 2009 / Published online: 18 September 2009

Abstract Carbon nanotube paper, sometimes referred to as bucky paper, is a random arrangement of carbon nanotubes meshed into a single robust structure, which can be manipulated with relative ease. Multi-walled carbon nanotubes were used to make the nanotube paper, and were subsequently modified with platinum using an electroless deposition method based on substrate enhanced electroless deposition. This involves the use of a sacrificial metal substrate that undergoes electro-dissolution while the platinum metal deposits out of solution onto the nanotube paper via a galvanic displacement reaction. The samples were characterized using SEM/EDS, and Hall-effect measurements. The SEM/EDS analysis clearly revealed deposits of platinum (Pt) distributed over the nanotube paper surface, and the qualitative elemental analysis revealed co-deposition of other elements from the metal substrates used. When stainless steel was used as sacrificial metal a large degree of Pt contamination with various other metals was observed. Whereas when pure sacrificial metals were used bimetallic Pt clusters resulted. The co-deposition of a bimetallic system upon carbon nanotubes was a function of the metal type and the time of exposure. Hall-effect measurements revealed some interesting fluctuations in sheet carrier density and the dominant carrier switched from *N*- to *P*-type when Pt was deposited onto the nanotube paper. Perspectives on the use of the nanotube paper as a replacement to traditional carbon cloth in water electrolysis systems are also discussed.

Keywords Carbon nanotube paper · Platinum · Hall measurements · Substrate enhanced electroless deposition · Membrane electrode assembly

Introduction

Interest and research with nanotubes continues to receive great attention worldwide. The unique physical–chemical properties due to the high aspect ratios and unique atomic arrangements are some of the general intrinsic factors that continue to drive new innovative applications. Carbon nanotubes (CNT) are by far the most studied and varied in terms of innovative application [1]. For example, Pande et al., demonstrated an effective electromagnetic shield using a polymer composite of CNT and poly methyl methacrylate, whereas Riggio et al. assembled an effective drug delivery system using CNT arrays, and in contrast Liu et al. successfully confined gallium inside CNT and demonstrated the efficacy of a nano-thermometer [2–4]. Besides electromagnetic shielding, and drug delivery applications, CNT have been used in electrochemical analytical and energy conversion systems, numerous biomedical applications, next generation electronic devices, and in diverse nano-composites [5–8].

CNT can be simply described as either one (single walled CNT), two (double-walled CNT), or more (multi-walled CNT) graphene sheets wrapped around a central hollow core. This arrangement of sp2 hybridized carbon atoms endows these materials with some fascinating tunable physical chemical properties. For example, chemical

L. Petrik (✉) · P. Ndungu
Environmental and Nanosciences Group,
University of the Western Cape, Bellville, South Africa
e-mail: lpetrik@uwc.ac.za

E. Iwuoha
Sensor Lab, Department of Chemistry,
Faculty of Natural Sciences, University of the Western Cape,
Bellville, South Africa

alteration of single-walled CNT has been shown to change the electronic properties; specifically, the band gap was found to shrink with degree of OH functionalization [9] and the exceptional thermal properties have been recently measured [10]. Although CNT have excellent structural properties and extremely interesting physical–chemical peculiarities, they remain difficult to exploit; however, Bucky paper offer a possible method to take advantage of CNT unique properties and allow ease of manipulation.

The term bucky paper was initially used to refer to a robust free standing mat of intertwined randomly arranged single-walled carbon nanotubes (SWCNT) [11, 12]. Eventually the term was also used to refer to similar arrangements of double [13] and multi-walled carbon nanotubes (MWCNT), and in time the phrase carbon nanotube paper was introduced and used interchangeably in the literature [14]. Baughman et al. [15] initially reported on the potential to utilize such a free standing structure/mat in an electrochemical based application, most notably as an actuator.

Interest and study on the utilization of carbon nanotube paper made from MWCNT has grown over the years. Recently Xu et al. investigated the mechanical properties of MWCNT papers, and compared pristine nanotube papers with those modified with polyvinyl alcohol, polyvinyl pyrrolidone, or polyethylene oxide. They found that the tensile strength and Young's modulus increased from 5 and 785 MPa for pristine nanotube paper to 96.1 and 6.23 GPa for nanotube paper infiltrated with polyvinyl alcohol, which was the polymer that gave the best results [16].

In terms of electrical properties various groups have reported on the excellent conductive nature of MWCNT papers. Xu et al. [16] reported an electrical conductivity of 1.0×10^4 S/m, but found that the conductivity of their nanotube papers varied slightly with the pre-treatment reflux temperatures. Using various mixtures of SWCNT with MWCNT or vapor grown carbon nanofibers (VCNF), Park et al. found that the conductivity for nanotube papers mixed with MWCNT and VCNF was 1.0×10^4 and 0.1×10^4 S/m, respectively. These values were lower than the samples consisting of random (1.40×10^4 S/m) and aligned SWCNT (3.33×10^4 S/m) only [17]. When comparing nanotube papers made of aligned MWCNT and randomly orientated MWCNT, Pengcheng et al. found that the electrical conductivity was 2.0×10^4 and 1.5×10^4 S/m, respectively [18].

Recently, MnO_2 nanowires were electrodeposited onto MWCNT papers. The resulting nano-composite had excellent flexibility, high-capacitance, and a long life cycle, making these materials an excellent candidate for flexible and thin super-capacitors [19]. In terms of altering the properties of MWCNT papers, Kakade et al. [20] demonstrated that the wetting properties of the paper could be changed from a superhydrophobic surface, produced by ozonolysis, to a superhydrophilic surface using an electric field.

Carbon supports are often used to stabilize electrocatalysts that may be applied in fuel cell or electrolyser polymer electrolyte membrane (PEM) electrode systems. Carbon supports offer several advantages in this regard; such as, the surface area of the catalyst is increased, uniform, and high dispersion of the catalyst at high loadings (>30%), excellent electronic conductivity and chemical stability, and the carbon substrate increases the stability of the catalytic particles and prevents agglomeration [21–23]. The size of nanophase platinum group metal (PGM) electrocatalysts raises significant challenges in stabilization. Transition and noble metal nanoparticles typically have high surface free energies, and therefore tend to agglomerate to reduce their surface area. Stabilization of nanosize metal particles can be achieved via deposition on to the surface of supports which can provide favorable metal-support interactions. The smaller the particle the more its physical properties and morphology can be affected by these interactions [23, 24].

The requirements of a support for an active electrocatalyst are rigorous. It must provide structural, conductive, and durable support for the active metal particles. Aggregation alters the volume, particle size, particle size distribution, porosity, and surface area of materials. Changes in surface area and volume by agglomeration or aggregation may influence the chemical reactivity of nanophase electrocatalysts [25]. Metal particle size distribution is largely influenced by the metal-support interaction and electrical charging of the particles has a significant effect on the predicted agglomeration rates [23, 24]. By far the most common support materials used in PEM fuel cells are carbon based, out of which carbon nanotubes have received the largest amount of attention in terms of research activity [26–29].

Qu and Dai [30] reported a substrate enhanced electroless deposition (SEED) procedure of metal nanoparticles on carbon nanotubes. This procedure is a simple galvanic displacement reaction and could facilitate the large scale production of nanoparticle coated carbon nanotubes. According to Choi et al. [31] a single wall nanotube has a reduction potential of +0.5 V versus SHE (standard hydrogen electrode) and these authors were able to successfully deposit Pt (+0.775 V versus SHE) as nanoparticles through spontaneous reduction of the metal ions by the nanotubes. In the SEED procedure of Qu and Dai [30] it was shown that metal ions even with a lower reduction potential than that of a conducting carbon nanotube can be reduced onto the support without an additional reducing agent. In this reaction the nanotube acts as cathode for

reducing the metal ion in solution whereas a chosen metal substrate acts as anode where the metal substrate's atoms are oxidized and displaced into solution [30].

We present the use of CNT paper as a substrate for the electroless deposition of platinum without the use of additional reducing additives (liquids or gases), and report on Hall measurements on the CNT paper modified with platinum.

Experimental

Synthesis and Treatment of CNT

CNT were prepared according to methods developed by Vivekchand et al. [32]. In brief, a mixture of a ferrocene–toluene (20.00 g L^{-1}) solution was nebulized, using ultrasound, and fed into a quartz tube located inside a tube furnace and maintained at a temperature of 900 °C. Ar was used as the carrier gas at a flow rate of 500 cm^{-3} min^{-1}. The nebulizer frequency was 1.6 MHz and the total reaction time was 45 min. Separate samples of CNT were synthesized under the same conditions using a solution of ferrocene in benzene (20.00 g L^{-1}).

For the purification and surface chemical modification, 0.2 g of CNT were weighed and placed into a round bottomed flask fitted with a thermostat and thermometer, where after 100 mL mixture of a sulfuric acid and nitric acid (2:3 ratios by volume of concentrated sulfuric acid (98%) and concentrated nitric acid (55%), was carefully added into the flask. The CNT were heated under reflux for 3 h, and after the mixture had cooled the CNT were gravity settled and the acid supernatant poured off where after the CNT were mixed with 500 mL of de-ionized water, and recovered. The recovery step used filter paper, a Buchner filtration system, and the CNT were washed until the rinse water had a pH of 6–7 as determined by indicator paper. CNT were then dried in an oven at 100 °C overnight.

After acid washing a portion of the CNT were processed into a dense felt or "CNT paper" by vacuum filtration of a CNT suspension in deionized water onto a 45 μm cellulose acetate filter and in situ drying upon the filter in an adaptation of the method described by Vohrer et al. [33]. The CNT suspension used, had a mass/volume concentration of 10 mg/mL, and the total volume used was ~50.0 mL.

Pt Deposition on to CNT Paper

A specific size and weight of stainless steel mesh or foil (99.99% lead, iron, and aluminum foil, respectively) was clipped tightly with a plastic covered paper clip to a pre-weighed piece of CNT paper. The CNT paper was suspended into a chloroplatinic solution with specific molar concentration of 0.01 M (0.5216 g in 100 mL), for various times, e.g., either 10 or 20 min. All samples were made in replicates. Different times of deposition were followed for each foil so that there were two variables that were altered for each system-time of deposition and type of metal foil. The foils were selected on the basis of their reducing ability (i.e., each metal coupled with Pt is thermodynamically favorable) based upon the respective $E^{\emptyset}$ (volts):

$$\text{Al: } E^{\emptyset} = -1.66 \text{ (highest); Fe : } E^{\emptyset} = -0.44 \text{ (intermediate); Pb : } E^{\emptyset} = -0.13 \text{ (lowest).}$$

Characterization

Samples were studied using Transmission Electron Microscopy (TEM, Hitachi H-800 EM, 200 kV, 20 μA), X-ray Diffractometry (XRD, Bruker AXS D8 Advance, Cu Kα ($\lambda = 1.5418$), 0.05° min^{-1}), total surface area and porosity by N_2-adsorption at −196 °C (77 K) (Micromeritics ASAP 2010, 20 mg sample), and Scanning Electron Microscopy with energy dispersive spectroscopy (EDS).

Hall mobility and resistivity was measured using a Lakeshore 7704 system with HMS Matrix 775 control instrument sample Module Model 75013SCSM (max 100 V) and a Sample Module Model 75013SCSM to apply the magnetic field (with a maximum of 10.8 Gauss). The 1 cm^2 electrode, CNT or Pt/CNT paper, was carefully trimmed and mounted on thin cardboard to ensure flatness and then mounted onto the Lakeshore sample holder (part number 750SC10-50) with "solvent and acid free water soluble glue" (Henkel Pritt). The electrical contact was made by placing small ohmic contacts on the four corners of the supported film using silver conductive ink (DuPont Silver paint 5000). The contacts were hand painted between each corner of the 1 cm^2 electrode and silver contact points 1, 2, 3, and 4 on the Lakeshore sample holders. Mounted samples were cured at 70 °C in a hot air oven for 30 min to ensure contact dryness. Manual resistance measurements were firstly obtained to check the integrity of contacts according to the Van der Pauw geometry which is geometry independent. Connections were made according to the (R12,12; R23,23; R34,34; and R41,41) configuration for each prepared electrode after mounting in a Lakeshore sample holder and a voltage applied between each terminal successively. The Van der Pauw geometry was used for IV curve measurement starting at −1.0 to 1.0 mA with a step size of $I = 0.1000$ mA and a dwell time of 5 s. Thereafter a variable field measurement was obtained for each sample between 10 and 1 kG at a step size of 1 kG and dwell time of 10 s at a current of 1 mA. The mode chosen was linear sweep with field reversal and geometry A + B to minimize any lack of symmetry.

Results and Discussion

Characterization of Purified CNT

After purification and surface chemical modification by acid treatment, the impurities in CNT were removed and little remaining Fe from the ferrocene catalyst could be detected by energy dispersive analysis (EDS). XRD analysis (not shown) of pre-treated CNT showed that after acid washing the XRD pattern for CNT contained the four characteristic diffraction peaks for crystalline graphite at *t* 26.5, 42.4, 54.7, and 77.4° 2 theta, namely of (220), (100), (004), and (110), respectively. The acid washed CNT had a N_2 BET surface area of 49 $m^2\ g^{-1}$ of which only 4 $m^2\ g^{-1}$ reported to the microporous internal area of the CNT as the surface area of CNT are made up of inter-tubular pores and intra-tube pores.

TEM micrographs (not shown) of un-treated carbon nanotubes, and acid treated carbon nanotubes indicated that the CNT were not uniform in dimensionality. However, this should not be a problem in the application of these materials as catalyst support, since uniformity of the support is not a critical requirement. The HRTEM images (Fig. 1) show that the CNT were multi-walled and the acid washing damaged the CNT wall, which is consistent with previous results reported in the literature [34, 35]. The acid treatment was sufficient to remove the metal catalyst to a significant degree but not completely, and is attributed to the inability of the acid to reach the encapsulated iron (Fig. 1b) within the CNT; hence the acid washing technique used was not sufficient to remove all the metal catalyst impurity.

CNT Paper Analysis

The SEM of CNT processed into CNT paper (Fig. 2) shows that the void spaces or "pores" between the matted CNT fibers are in the order of microns, and these void spaces can be considered as macropores, and are areas through which gas diffusion can freely take place.

The CNT in turn have an internal mesopore structure which was evident in the HRTEM (Fig. 1a), and as a result the processed CNT material contains mesoporosity. When comparing CNT paper with conventional carbon paper (Fig. 2a, b), the SEM micrographs clearly show that the overall macroporosity of the CNT paper is significantly greater (large number of small macropores) than the carbon paper and the external surface area is much greater. The physical differences in the size of the individual CNT compared to the carbon fibers are the direct cause behind this observation, and is of interest in PEM systems (fuel cells or water electrolysis) where the overall surface area of the gas diffusion layer (GDL) will be increased considerably. Additionally, the use of the CNT paper as support substrate for Pt should promote an increase of the dispersion of the Pt electrocatalyst because of the much higher effective surface area that is available to support the catalyst. Moreover, the conductive contacts between phases necessary to develop the three phase boundary in the PEM electrode should be highly improved.

Characterization of Electroless Deposited Pt on CNT Paper

Excessive deposition of Pt upon the carbon nanotube paper was observed when utilizing stainless steel as a sacrificial

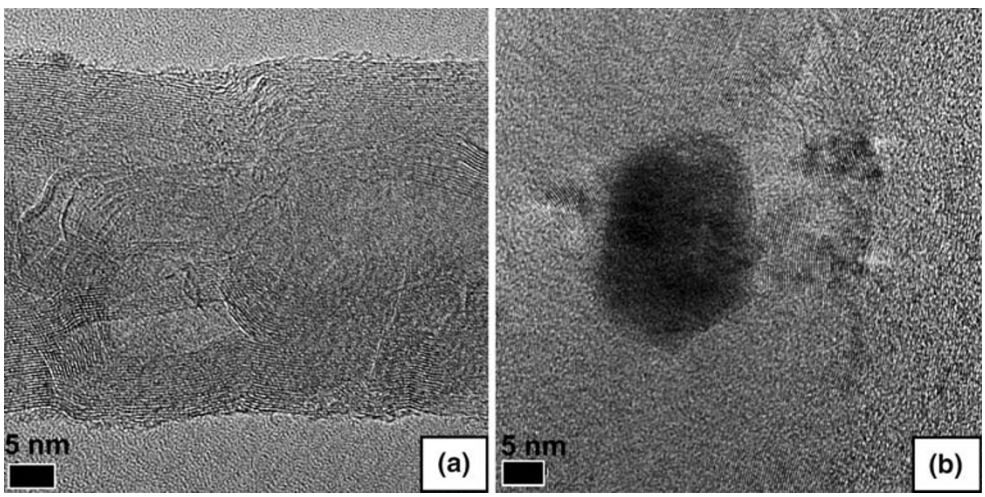

Fig. 1 HRTEM images of acid washed CNT prepared by ferrocene–toluene method; image **a** shows a MWCNT with imperfect pore walls, and **b** is an example of an encapsulated Fe impurity in CNT

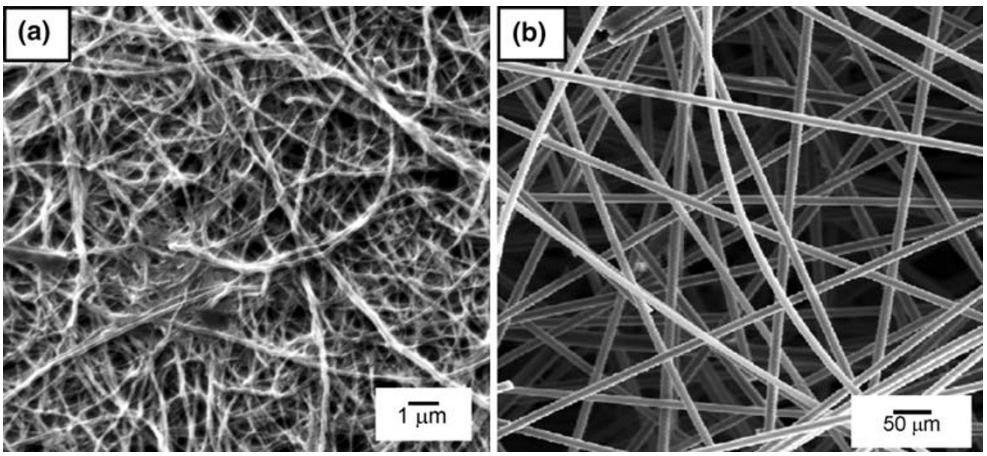

Fig. 2 SEM micrographs of CNT paper (**a**) and ordinary carbon paper (**b**)

anode (Fig. 3), and is due to the length of time (1 h) initially used.

The long deposition time resulted in complete coverage of the MWCNT with Pt deposits at the surface of the nanotube paper. The deposits were spherical, and completely covered the length of the MWCNT sidewalls. This result is similar to those that were reported by Qu and Dai [30]. Along the individual MWCNT, the deposits are similar in size, and this is most likely due to fast nucleation of nanoparticles independent of any defect sites on the MWCNT, and faster growth of smaller relative to larger particles due to diffusion limited movement of Pt salt [30]. Moreover, significant co-deposition of various components derived from the stainless steel was detected by EDS (figure not shown). Because of the impurities observed when using stainless steel mesh as sacrificial electrode; the use of relatively pure foils was implemented thereafter to promote the galvanic displacements, and to produce pure bimetallic catalyst systems. Much shorter times were applied to minimize the degree of wastage of Pt in the bulk, and as an attempt to directly form nano sized metal deposits on the CNT paper.

After Pt deposition, using 99.99% pure Al, Pb, or Fe foils, respectively, the CNT paper increased in mass (Fig. 4).

The replication was poor mainly due to incomplete recovery of the CNT paper from the solution in some cases. Generally the shorter time caused less metal to deposit in the case of Al and Fe foils, but only with the Al foil did the mass% increase double as the time was doubled. In the case of Fe no measurable increase in mass of the CNT substrate occurred during the first 10 min, possibly indicating a slow galvanic displacement reaction for this system. However, this was not true of the Pb foil where both

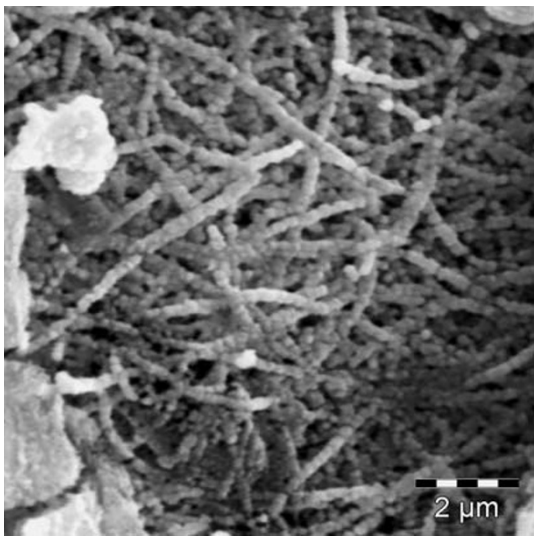

Fig. 3 Galvanic displacement deposition of Pt (8 h) on CNT paper using stainless steel as sacrificial anode

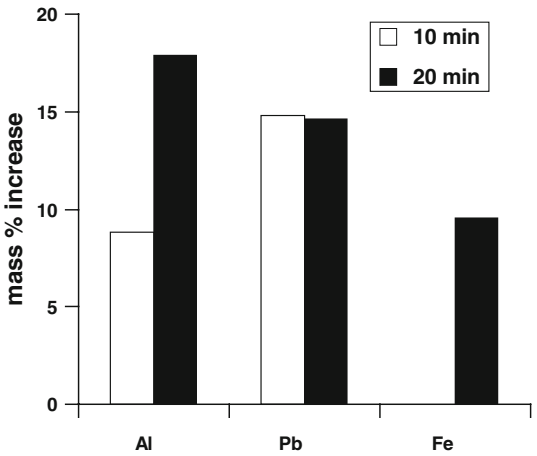

Fig. 4 Mass% increase of CNT paper after Pt deposition over 10 and 20 min, with the Fe foil no measurable increase was seen after 10 min

times applied allowed a similar increase in mass of the CNT substrate. This may indicate that with the Pb foil, the initial stages of nucleation and growth occur sometime before 10 min (shorter deposition time), and equilibrium has been reached ahead of the 10 min stop time.

EDS Analysis of Electroless Deposited Pt on CNT Paper

EDS was performed after SEM images were obtained to determine the atom% Pt and establish whether any other metal had been co-deposited during the galvanic displacement reaction. The highest Pt loading on the CNT paper was observed in the case of the Fe foil after 10 min. More Pt was deposited on the CNT paper in the first 10 min in the case of the Al, Pb, and Fe foils, whereas less Pt was deposited during the longer deposition time of 20 min. However, a large variability was found in the amount of Pt deposited on different areas of the CNT paper in most cases (Fig. 5). A significant % of the metal deriving from the foil used in the displacement reaction was co-deposited, thus leading to bimetallic deposits particularly after the longer deposition period in the case of Al foil and in the case of Pb within the first 10 min as shown in Fig. 5. As the metals differed greatly in MW therefore the atom% is presented in Fig. 5.

As there was significant inhomogeneity in the Pt dispersion on the CNT as can be observed by SEM (Fig. 6a–f), the EDS values of the elemental composition of samples are mainly qualitative. Morphological characterization was performed using SEM and selections of the micrographs are presented in Fig. 6.

From the EDS results of the elemental composition of the samples prepared using Al foil the degree of co-deposition of Al ranged from 1.5 to nearly 3 atom% depending on the deposition time of 10 and 20 min, respectively and a small Fe contaminant of between 0.24 and 0.86 atom % was also observed which was unexpected as the metal foils used as sacrificial electrodes were 99.99% pure; however, from Fig. 1 this is most likely due to encapsulated Fe

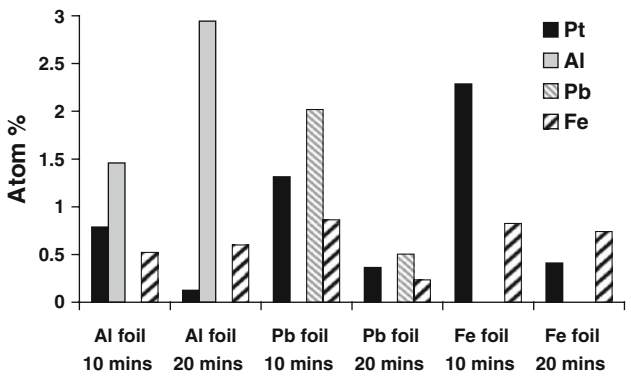

Fig. 5 Atom% of bimetallic deposits on CNT

catalyst particles. In the case of the Fe foil, about 0.8 atom% Fe was co-deposited with the Pt. In the case of Pb foil 2 atom% of Pb was co-deposited with the Pt and more was apparently co-deposited at the shorter deposition time of 10 min than at the longer time of 20 min. This variability in elemental composition determined by EDS may be due to the inhomogeneity of the metal deposition upon the CNT that was observed by SEM (Fig. 6) and these results should be treated with caution as they are based upon the analysis of very small areas. From the SEM results in Fig. 6, the use of the Pb foil resulted in relatively consistent and homogeneous Pt deposition and few large Pb containing Pt clusters formed. In addition, the deposition time used did not make a large difference in the results obtained and the deposition was also more evenly dispersed. These results highlight that the compositional analysis by EDS is merely qualitative.

In the galvanic displacement the substrate metal acts as a sacrificial anode and donates an electron to the CNT and in the process is oxidized and displaced into solution [30]. However, from the results presented it can be seen that the displaced metal ions then compete with the Pt ions in solution and thus are co-deposited upon the CNT with the Pt. This is obviously a result of the increasing concentration of the metal ions in solution over time. It appears from the data that the longer the contact time, the more the subsidiary metal predominates in the co-reduction and deposition reaction, particularly in the case of Al (E^{ϕ} −1.66), whereas for the metals with lower E^{ϕ} such as Fe (−0.44) or Pb (−0.13) this trend was not significant in the time of the reaction.

Characterization of Electroless Deposited Pt on CNT Paper Using a Hall Measurement System

Resistivity of the CNT paper was initially investigated by a four point technique using a Hall measurement system (Ecopia HMS 3000, Korea). The CNT paper had a low resistivity of approximately 0.033 Ω, although this value is close to similar measurements in the literature [36], it was not as low as the typical graphite resistivity that ranges from 9 to 40 μΩm; this difference can be attributed to the contact resistance between individual nanotubes, and the CNT paper and the silver paste used to connect the sample to the hall measurement system.

Initial electronic characteristics of the composite Pt/CNT paper electrode materials formed by galvanic displacement using stainless steel are presented in Table 1 and Fig. 7.

The sheet resistance R_S is determined by use of the Van der Pauw resistivity measurement technique [37]. A resistivity and a Hall measurement are needed to determine the mobility μ and the sheet density n_s (ASTM method F76, 2000).

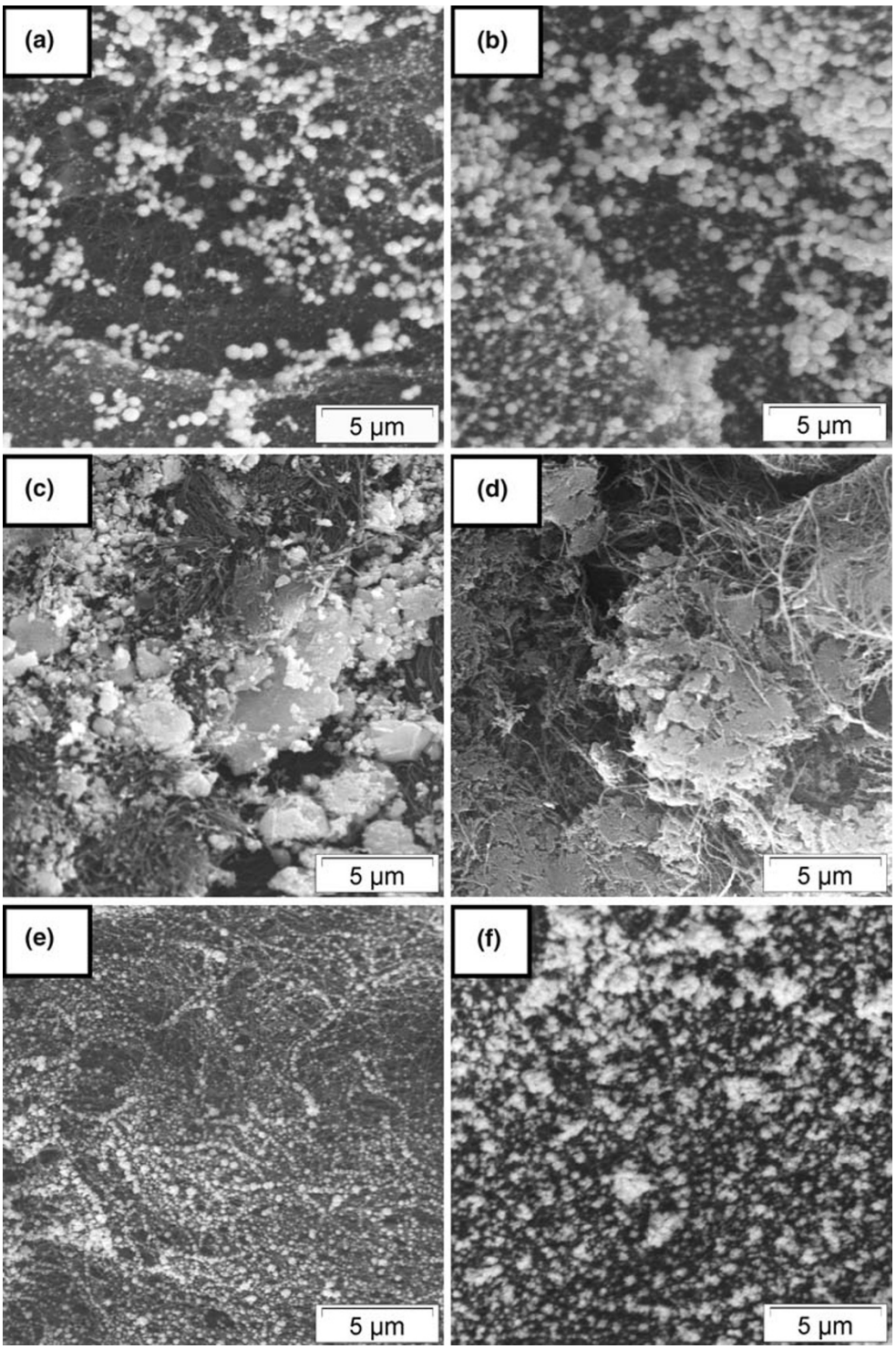

Fig. 6 SEM micrographs of CNT paper with Pt deposition using Al (10 (**a**) and 20 (**b**) min deposition), Fe (10 (**c**) and 20 (**d**) min deposition) and Pb (10 (**e**) and 20 (**f**) min deposition) foils

The Hall measurement, carried out in the presence of a magnetic field, yields the sheet carrier density n_s and the bulk carrier density n if the conducting layer thickness of the sample is known. The carriers can be a positive or negative carrier type. Conventionally in a dry semiconducting material the positive carriers are "holes" and the negative carriers, electrons. In electrolytes both carriers can be ions. The variability of resistance between contact pairs was not significant, thus electrical contacts were of reasonable quality.

Table 1 Resistance of Pt/CNT paper

Sample	R12,12	R23,23	R34,34	R41,41
Blank paper substrate (G Ω)	6.8	12.8	7.5	10.0
CNT paper (Ω)	49.57	49.65	49.39	49.30
CNT paper + Pt (Ω)	60.61	102.23	102.58	61.54

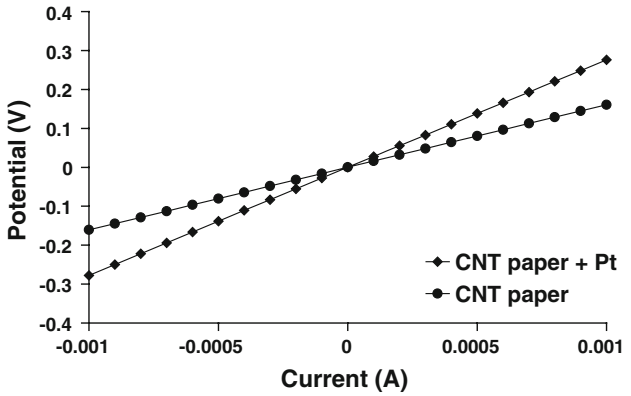

Fig. 7 IV curves for the CNT paper and CNT paper + Pt

The IV curves obtained using the Hall measurement system for CNT paper and CNT paper coated with Pt nanoparticles using stainless steel as sacrificial anode are shown in Fig. 7. Although this sample has the largest amount of Pt deposit, it also had a more uniform coverage along the length of the individual CNT, and was thus used to compare unmodified CNT paper and modified CNT paper. The very low potentials observed at the applied currents of CNT paper (0.1604 V at 1 mA) and CNT paper + Pt (0.2759 V at 1 mA) demonstrated the excellent conductive characteristics of these materials.

The sheet resistivity of CNT paper compared to the Pt containing CNT paper is shown in Fig. 8. The sheet resistivity of a typical carbon cloth was 0.99 Ω cm^{-1} (not shown). The sheet resistivity of CNT paper was 0.35 Ω cm^{-1} compared to CNT paper + Pt which was 3.75 Ω cm^{-1}, thus a small increase in sheet resistivity was observed when the Pt was incorporated into the CNT paper. The use of a highly electroconductive CNT substrate thus had a significant effect upon lowering the overall sheet resistivity but deposition of Pt increased the sheet resistivity, which highlights that the main current pathways are located near the outer layers of the individual CNT, and thus one would expect an increase when modifying these outer layers.

The sheet carrier density of the CNT paper and CNT + Pt samples is shown in Fig. 9, and was generally similar and of the same order of magnitude as carbon cloth samples, thus neither of the conductive substrates made a significant difference to the sheet carrier density characteristics overall.

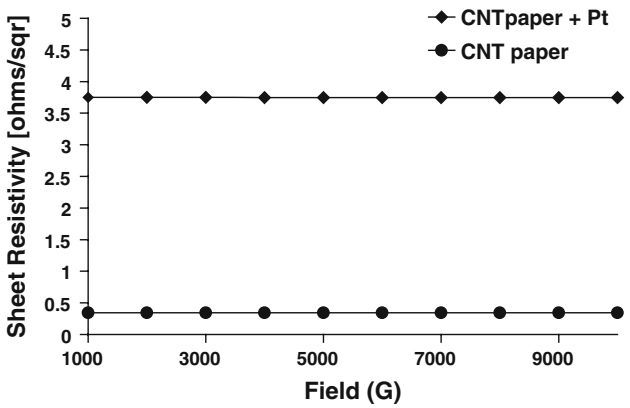

Fig. 8 Sheet resistivity of CNT paper compared to CNT paper + Pt

An anomalous fluctuation was observed in the case of the CNT paper + Pt sample during the application of the magnetic field and this may be due to instability caused by mechanical movement or displacement of the Pt particles relative to the CNT under the applied magnetic field. The galvanic displacement method deposited not only Pt but other metals from the sacrificial anode; the presence of these metals may have caused a magnetic interaction. It is unlikely that the anomalous fluctuation is due to quantum confinement phenomena, since these are usually observed at low temperatures and/or high magnetic fields [38].

The Hall mobility of the CNT based electrode samples (Fig. 10) were on the same order of magnitude as those of the carbon cloth samples and the Hall mobility was between one and two orders of magnitude higher than the paper substrates. It is interesting to observe that deposition of Pt upon CNT reduced the overall hall mobility, which may indicate the role of Pt as a recombination site and supports the possibility of quantum confinement of charge carriers by Pt nanoparticles [39].

The average Sheet Hall Coefficients of the film samples are tabulated in Table 2 and the dominant carrier is shown

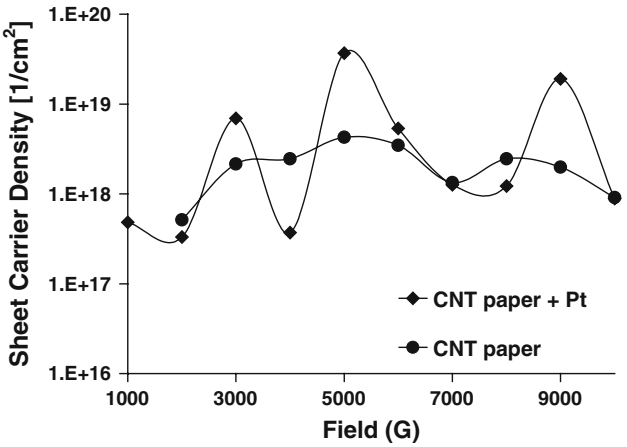

Fig. 9 Sheet carrier density for CNT paper and CNT paper + Pt

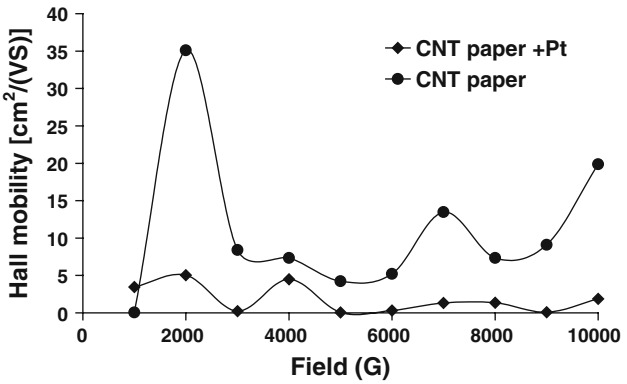

Fig. 10 Hall mobility of CNT paper samples

for each case. As the sheet hall coefficient is reduced and values approach zero or become negative the sheet becomes more electroconductive.

The CNT paper sample switched from *n*- to *p*-type carrier upon deposition of the Pt, indicating that electron conduction changed to hole conduction upon deposition of the Pt. This is a unique result and should be further investigated. Le et al. [40] observed that their multi-walled CNT films were *p*-type carriers, this difference between our CNT paper and that reported by Le et al., can be attributed to multiple factors including difference in synthesis of the CNT (radio frequency excitation CVD versus conventional thermal CVD), difference in treatment of the CNT (different chemical treatment of CNT has been shown to dope and alter the electronic properties of CNT [40]), and the difference in characteristics of the CNT (length, diameter, number of shells, etc.).

It is possible that Pt becomes a site for carrier recombination, thus the Pt may capture the charge carriers and build up a charge as it can easily take up the charge but cannot transfer it further via a chemical reaction due to the lack of reactant in the experimental system used for the Hall measurements. This may be indicative of quantum confinement of carriers in the nanoparticles of Pt dispersed upon the CNT [39]. *N*-type carriers, which are normally found in metallic conductors, allow the transfer and flow of electrons. In the cases where *p*-type carriers dominated it may be that the electron flows were impeded due to lack of connectivity between catalyst particles. Adequate connectivity between catalyst particles or agglomerates would be required for a percolation pathway threshold. An optimum distribution and density is required for continuous electronic contact. Thus, the Hall measurement system can be used to determine surface electronic properties of the CNT paper modified with platinum, in terms of change in carrier type. In turn, this maybe extended to monitoring loading versus carrier type transition; however, for electrochemical applications, this system will need to be coupled with conventional electrochemical characterization techniques to establish the effect carrier type transitions have on electrocatalytic activity of interest.

Table 2 Average sheet hall coefficient

Sample	Average sheet hall coefficient ($cm^2\ C^{-1}$)	Dominant carrier
Bond paper blank	2.76E + 09	P
Carbon cloth	−3.24	N
CNT paper	−1.383	N
CNT paper + Pt	1.372	P

In terms of electrochemical activity, CNT in general have been widely investigated and shown to have superior characteristics when compared to other forms of carbon [8, 41]. Interest in Pt/CNT systems for PEM systems is an intensive area of R&D [42], and similar studies on the CNT paper systems used in the current work would be of immense interest. Such investigations are under way and will be presented in a future publication.

Conclusions

CNT paper was prepared using a simple vacuum filtration technique from processed MWCNT, which were synthesized using a nebulized spray pyrolysis method. The CNT paper was subsequently used as a substrate to deposit Pt via a galvanic displacement technique. This is a simple procedure that can be optimized and used to eliminate the extensive processing that is required for stabilization of nanophase Pt based catalysts on porous matrixes, and is an alternative and simple method for the preparation of GDL for membrane electrode assemblies. The use of CNT paper as a substrate to support electrocatalysts highlights the possibility of using an alternative GDL for membrane electrode assemblies. This procedure would thus eliminate a large amount of processing and illustrates a route to easily form a series of GDL incorporating nanophase Pt containing electrocatalysts by use of the galvanic displacement deposition technique. The results of the galvanic displacement showed that it is possible to directly deposit Pt and a second metal on CNT paper substrates to form bimetallic electrocatalysts and that the deposition rate and bimetallic nature of the metals deposited were influenced by the sacrificial anode metal type as well as by the contact time.

Hall measurements showed that CNT paper and CNT paper modified with Pt had excellent electrical conductivity. The sheet resistivity increased slightly when the CNT paper was modified with Pt, and an anomalous fluctuation in the sheet carrier density was observed with the CNT paper modified with Pt. At this time, this is attributed to

magnetic interaction due to the presence of iron in the CNT paper or in Pt deposits; however, whether this has to do only with the nature of the modified CNT will need to be investigated further.

The modification of the CNT paper with Pt switched the CNT substrate from *n*- to *p*-type carrier, demonstrating the effect the metal electrocatalyst may have upon carrier properties of a GDL prepared by this route. Modification of CNT by deposition of metals can alter electronic properties, and the presence of Pt nanoparticles on the CNT created alternative current pathways, which due to the nature of the Pt deposits switched the CNT substrate from *n*- to *p*-type carrier.

Acknowledgments The authors would like to acknowledge Professor Britton and Professor Härting for aid with the Hall measurements, Professor Knoesen for fruitful discussions on the Hall Effect, and Miranda Waldron and Mohammed Jaffer for help with SEM and TEM observations respectively. The authors are also grateful to the National Research Foundation of South Africa for financial support.

References

1. C. Yan, J. Liu, F. Liu, J. Wu, K. Gao, D. Xue, Nanoscale Res. Lett. **3**, 473 (2008)
2. S. Pande, B.P. Singh, R.B. Mathur, T.L. Dhami, P. Saini, S.K. Dhawan, Nanoscale Res. Lett. **4**, 327 (2009)
3. C. Riggio, G. Ciofani, V. Raffa, A. Cuschieri, S. Micera, Nanoscale Res. Lett. **4**, 668 (2009)
4. Z. Liu, R. Zheng, K.R. Ratinac, S.P. Ringer, Funct. Mater. Lett. **1**, 55 (2008)
5. G.G. Wildgoose, C.E. Banks, R.G. Compton, Small **2**, 182 (2006)
6. Y. Lin, S. Taylor, H. Li, K.A.S. Fernando, L. Qu, W. Wang, L. Gu, B. Zhou, Y.-P. Sun, J. Mater. Chem. **14**, 527 (2004)
7. M.P. Anantram, F. Léonard, Rep. Prog. Phys. **69**, 507 (2006)
8. M. Terrones, Annu. Rev. Mater. Res. **33**, 419 (2003)
9. S.H. Lim, J. Lin, L. Liu, H. Pan, H.L. Pan, W. Ji, Y.P. Feng, Z. Shen, Funct. Mater. Lett. **1**, 1 (2008)
10. J. Guo, X. Wang, D.B. Geohegan, G. Eres, Funct. Mater. Lett. **1**, 71 (2008)
11. A. Rinzler, J. Liu, H. Dai, P. Nikolaev, C. Huffman, F. Rodrıguez-Macıas, P. Boul, A. Lu, D. Heymann, D. Colbert, R. Lee, J. Fischer, A. Rao, P. Eklund, R. Smalley, Appl. Phys. A **67**, 29 (1998)
12. J. Liu, A. Rinzler, H. Dai, J. Hafner, R. Bradley, P. Boul, A. Lu, T. Iverson, K. Shelimov, C. Huffman, F. Rodriguez-Macias, Y.-S. Shon, T. Lee, D. Colbert, R. Smalley, Science **280**, 1253 (1998)
13. H. Muramatsu, T. Hayashi, Y. Kim, D. Shimamoto, Y. Kim, K. Tantrakarn, M. Endo, M. Terrones, M. Dresselhaus, Chem. Phys. Lett. **414**, 444 (2005)
14. P.G. Whitten, G.M. Spinks, G.G. Wallace, Carbon **43**, 1891 (2005)
15. R.H. Baughman, C. Cui, A.A. Zakhidov, Z. Iqbal, J.N. Barisci, G.M. Spinks, G.G. Wallace, A. Mazzoldi, D. De Rossi, A.G. Rinzler, O. Jaschinski, S. Roth, M. Kertesz, Science **284**, 1340 (1999)
16. G. Xu, Q. Zhang, W. Zhou, J. Huang, F. Wei, Appl. Phys. A **92**, 531 (2008)
17. J.G. Park, S. Li, R. Liang, X. Fan, C. Zhang, B. Wang, Nanotechnology **19**, 185710 (2008)
18. D. Pengcheng, S. Changhong, L. WeiWu, S. Fan, Nanotechnology **19**, 075609 (2008)
19. S.-L. Chou, J.-Z. Wang, S.-Y. Chew, H.-K. Liu, S.-X. Dou, Electrochem. Commun. **10**, 1724 (2008)
20. B. Kakade, R. Mehta, A. Durge, S. Kulkarni, V. Pillai, Nano Lett. **8**, 2693 (2008)
21. P. Serp, M. Corrias, P. Kalck, Appl. Catal. A Gen. **253**, 337 (2003)
22. A.L. Dicks, J. Power Sources **156**, 128 (2006)
23. R. Ferrando, J. Jellinek, R.L. Johnston, Chem. Rev. **108**, 845 (2008)
24. E. Allen, P. Smith, J. Henshaw. Report no. AEAT/R/PSEG/0398 (2001). http://www.tanks.org/ttgdoc/AEAT-R-PSEG-0398.doc. Accessed May 2009
25. P. Simonov, V.A. Likholobov, *Catalysis and electrocatalysis at nanoparticle surfaces* (Marcel Dekker Inc., New York, 2003)
26. M. Uchida, Y. Fukuoka, Y. Sugawara, N. Eda, A. Ohta, J. Electrochem. Soc. **143**, 2245 (1996)
27. W. Li, W. Zhou, H. Li, Z. Zhou, B. Zhou, G. Sun, Q. Xin, Electrochim. Acta **49**, 1045 (2004)
28. J. Prabhuram, T.S. Zhao, C.W. Wong, J.W. Guo, J. Power Sources **134**, 1 (2004)
29. L.R. Jordan, A.K. Shukla, T. Behrsing, N.R. Avery, B.C. Muddle, M. Forsyth, J. Appl. Electrochem. **30**, 641 (2000)
30. L. Qu, L. Dai, J. Am. Chem. Soc. **127**, 10806 (2005)
31. H.C. Choi, M. Shim, S. Bangsaruntip, H. Dai, J. Am. Chem. Soc. **124**, 9058 (2002)
32. S.R.C. Vivekchand, L.M. Cele, F.L. Deepak, A.R. Raju, A. Govindaraj, Chem. Phys. Lett. **386**, 313 (2004)
33. U. Vohrer, I. Kolaric, M.H. Haque, S. Roth, U. Detlaff-Weglikowska, Carbon **42**, 1159 (2004)
34. C.H. Lau, R. Cervini, S.R. Clarke, M.G. Markovic, J.G. Matisons, S.C. Hawkins, C.P. Huynh, P.G. Simon, J. Nanopart. Res. **10**, 77 (2008)
35. P.-X. Hou, C. Liu, H.-M. Cheng, Carbon **46**, 2003 (2008)
36. A.K. Chatterjee, M. Sharon, R. Banerjee, M. Neumann-Spallart, Electrochim. Acta **48**, 3439 (2003)
37. L.J. Van der Pauw, Philips Tech. Rev. **20**, 220 (1960)
38. E. Jobiliong, J.G. Park, J.S. Brooks, R. Vasica, Curr. Appl. Phys. **7**, 338 (2007)
39. O.N. Hallback, A.-S. Zandvliet, H.J.W. Speets, E.A. Jan Ravoo, B. Reinhoudt, D.N. Poelsema, J. Chem. Phys. **123**, 397 (2005)
40. Z. Li, H.R. Kandel, E. Dervishi, V. Saini, Y. Xu, A.R. Biris, D. Lupu, G.J. Salamo, A.S. Biris, Langmuir **24**, 2655 (2008)
41. M. Pumera, Nanoscale Res. Lett. **2**, 87 (2007)
42. J.-H. Wee, K.-Y. Lee, S.H. Kim, J. Power Sources **165**, 667 (2007)